J. Am. Soc. Mass Spectrom. (2017) 28:452–460
DOI: 10.1007/s13361-016-1583-x

RESEARCH ARTICLE

Mechanistic Study of the Gas-Phase In-Source Hofmann Elimination of Doubly Quaternized Cinchona-Alkaloid Based Phase-Transfer Catalysts by (+)-Electrospray Ionization/Tandem Mass Spectrometry

Rong-Sheng Yang,[1] Huaming Sheng,[1] Katrina W. Lexa,[2] Edward C. Sherer,[3] Li-Kang Zhang,[1] Bangping Xiang,[1] Roy Helmy,[4] Bing Mao[1]

[1]Analytical Research and Development, Merck and Co. Inc., Rahway, NJ 07065, USA
[2]Process Research and Development, Merck and Co. Inc., Rahway, NJ 07065, USA
[3]Structural Chemistry, Merck and Co. Inc., Rahway, NJ 07065, USA
[4]Analytical Science, Merck and Co. Inc., Rahway, NJ 07065, USA

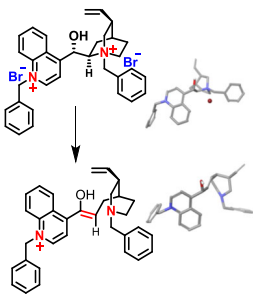

Abstract. An unusual in-source fragmentation pattern observed for 14 doubly quaternized cinchona alkaloid-based phase-transfer catalysts (PTC) was studied using (+)-ESI high resolution mass spectrometry. Loss of the substituted benzyl cation (R1 or R2) was found to be the major product ion $[M^{2+} - R_1^+$ or $R_2^+]^+$ in MS spectra of all PTC compounds. A Hofmann elimination product ion $[M - H]^+$ was also observed. Only a small amount of the doubly charged M^{2+} ions were observed in the MS spectra, likely due to strong Columbic repulsion between the two quaternary ammonium cations in the gas phase. The positive voltage in the MS inlet but not the ESI probe was found to induce this extensive fragmentation for all PTC diboromo-salts. Compound **1** was used as an example to illustrate the proposed in-source fragmentation mechanism. The mechanism of formation of the Hofmann elimination product ion $[M - H]^+$ was further investigated using HRMS/MS, H/D exchange, and DFT calculations. The proposed formation of **2b** as the major Hofmann elimination product ion was supported both by HRMS/MS and DFT calculations. Formation of product ion **2b** through a concerted unimolecular E_i elimination pathway is proposed rather than a bimolecular E2 elimination pathway for common solution Hofmann eliminations.

Keywords: Phase-transfer catalysts, Hofmann elimination, Mechanistic study, In-source fragmentation, DFT, (+)-ESI

Received: 22 September 2016/Revised: 4 December 2016/Accepted: 11 December 2016/Published Online: 18 January 2017

Introduction

Cinchona alkaloids are natural products found in the bark of trees of the genus *Cinchona*. Besides their well-known medicinal use, various cinchona alkaloids and their derivatives have been employed as key structural subunits in the synthesis of other complex natural products [1, 2]. Recently, a new class of cinchona alkaloid-based phase-transfer catalysts (PTC), which are quaternized at both the quinuclidine and quinoline nitrogens, were reported [3]. These catalysts demonstrated excellent reactivity and enantioselectivity in spirocyclization reactions [3].

Mass spectrometry (MS) has become a preferred analytical method for quaternary ammonium salts owing to its high specificity and sensitivity [4, 5]. Tandem mass spectrometry (MS/MS) is able to provide further molecular level structural information for individual ammonium ions [6, 7]. In early studies, the MS and MS/MS analysis of various mono-quaternary ammonium salts were done using different ionization techniques such as thermospray [8], fast atom bombardment (FAB) [9], and atmospheric pressure ionization (API) [10–15]. Generally, these reports have focused either on detection of the quaternary cation, or on selected reaction monitoring

Electronic supplementary material The online version of this article (doi:10.1007/s13361-016-1583-x) contains supplementary material, which is available to authorized users.

Correspondence to: Huaming Sheng; *e-mail:* huaming.sheng@merck.com

(SRM) of a characteristic transition through MS/MS. Only recently have a few mass spectrometric studies of surfactants, pesticides, and pharmaceuticals that have symmetric bisquaternary ammonium centers been reported [16–23]. Among these studies, most of the bisquaternary compounds display differing extents of in-source fragmentation in MS spectra, primarily driven by strong Columbic repulsion between the two charged sites [16, 17]. The distance between two preformed charged sites is essential to the stability of the doubly charged ion in the gas phase [16, 17]. In addition to observing the doubly charged ion M^{2+}, counter anion (A^-), and ion pair $[M^{2+} + A^-]^+$, the formation of an $[M - H]^+$ ion was observed as a minor product ion in the MS spectrum of a few symmetrical bisquaternary compounds. This was attributed to a gas-phase Hofmann elimination [16–20]. However, to the best of our knowledge, no previous study had focused on the mechanistic understanding of this reaction in the gas phase.

Mass spectrometry was employed in the present study for a series of novel PTC compounds. The two quaternary ammonium centers in each PTC compound make them an ideal model for the study of gas-phase Hofmann eliminations. As shown in Figure 1, all compounds contain three substituents: R_1 to R_3. Besides the expected doubly charged M^{2+} ions and common fragment ions $[M^{2+} - R_1^+$ or $R_2^+]^+$, all doubly charged PTCs exhibited a unique $[M - H]^+$ ion as the major product ion in the MS spectra. To better understand these observations, the in-source and MS/MS fragmentation patterns of the novel doubly quaternized cinchona alkaloid-based phase-transfer catalysts (with the general formula depicted in Figure 1) were further studied using electrospray ionization high resolution tandem mass spectrometry (ESI-HRMS/MS).

Experimental

Chemicals

All PTC related compounds were synthesized and fully characterized by NMR in a previous report [3]. All PTC was prepared as dibromo-salt. Deuterium oxide (D_2O) and deuterated trifluoroacetic acid-d (TFA-d) were purchased from Sigma Aldrich (St. Louis, MO, USA). All solvents used for LC/UV/MS analysis were of OPTIMA LC/MS grade purchased from Fisher Scientific (Pittsburgh, PA, USA).

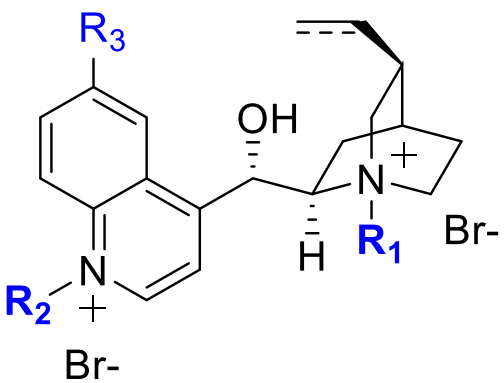

Figure 1. Cinchona-alkaloid based phase-transfer catalysts used in the present study

Mass Spectrometric Analysis

Mass spectrometric analysis was performed on a Waters Synapt G1 Q-ToF operating in positive or negative ion mode. Samples were dissolved in 100% ACN at the concentration of 0.1 mg/mL to avoid any possible anion exchange during ionization. To study potential solvent effect, samples were also dissolved in 50% ACN/water at the same concentration. Samples were introduced into the instrument using direct infusion at the flow rate of 20 μL/min. For the H/D exchange experiments, samples were dissolved in 50% ACN in D_2O. Source temperature and desolvation temperature were set at 130 °C and 350 °C, respectively. Nitrogen was used as both cone gas (40 L/h) and desolvation gas (600 L/h), and argon was used as the collision gas. The capillary voltage was set to 3 KV. A cone voltage of 5 V was applied. Leucine enkephalin was used as the lock mass (*m/z* of 556.2771) for accurate mass calibration and was introduced using the lock spray interface at 20 μL/min at a concentration of 0.5 μg/mL in 50% aqueous acetonitrile containing 0.1% formic acid. During mass spectrometric scanning, data were acquired in centroid mode from *m/z* 50 to 1000. For MS/MS fragmentation of target ions, collision energies ranging from 10 to 20 V were applied.

Computational Protocol

All calculations were performed with the Gaussian 09 package [24]. Geometry optimization, energy calculations, and transition state identification were carried out with density functional theory, using the M062X functional [25]. The LANL2DZ basis set [26–28] with an effective core potential was used for bromine, and the 6-31+G** basis set [29] was used for other atoms. Frequency analysis was conducted at the same level of theory in order to verify saddle points and obtain thermodynamic energy corrections without scaling at 298.15 K. Computed structures are illustrated using Maestro and Agui [30, 31].

Results and Discussion

MS Spectra of PTCs

Fourteen PTCs (**1**–**14**) were studied and their MS in-source fragment ions and relative abundances are summarized in Table 1. Compounds **1**–**12** were bisquaternized at both the quinuclidine and the quinoline nitrogens. Compounds **13**–**14** had only one quaternized center at the quinuclidine nitrogen. For bisquaternized compounds **1**–**12**, loss of the substituted benzyl cation R_1^+ or R_2^+ led to formation of $[M^{2+} - R_1^+$ or $-R_2^+]^+$ as the major product ions. The benzyl cations R_1^+ or R_2^+ were also observed as fragment ions. The relative abundances of the doubly charged ion M^{2+} was less than 30% for most doubly charged compounds. Lowering the cone voltage to 5 V

Table 1. All Ions of 14 PTC Compounds with Different R_1, R_2, and R_3 Groups are Listed with Their *m/z* Values and Relative Abundances in the MS Spectra. The In-Source Hofmann Elimination Product Ions are Marked in Red

PTC Compounds (MW)	Ions in MS Spectrum (*m/z* value and relative abundance)	PTC Compounds (MW)	Ions in MS Spectrum (*m/z* value and relative abundance)
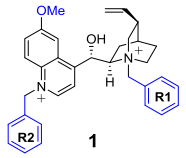 **1** (476)	$[M\text{-}H]^+$ (*m/z* 475, 28%) $[M^{2+}\text{- } R_1^+ \text{ or } R_2^+]^+$ (*m/z* 385, 100%)	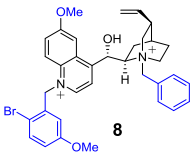 **8** (614)	$[M\text{-}H]^+$ (*m/z* 613, 20%) $[M^{2+}\text{-}R_1^+]^+$ (*m/z* 523, 100%) $[M^{2+}\text{-}R_2^+]^+$ (*m/z* 415, 8%) M^{2+} (*m/z* 307, 11%)
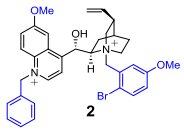 **2** (614)	$[M\text{-}H]^+$ (*m/z* 613, 18%) $[M^{2+}\text{-}R_1^+]^+$ (*m/z* 415, 100%) M^{2+} (*m/z* 307, 4%) R_1^+ (*m/z* 198, 45%)	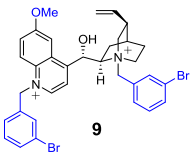 **9** (664)	$[M\text{-}H]^+$ (m/z 663, 30%) $[M^{2+}\text{- } R_1^+ \text{ or } R_2^+]^+$ (*m/z* 495, 100%) M^{2+} (*m/z* 332, 34%) R_1^+ or R_2^+ (*m/z* 168, 80%)
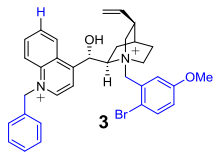 **3** (584)	$[M\text{-}H]^+$ (*m/z* 583, 25%) $[M^{2+}\text{-}R_2^+]^+$ (*m/z* 493, 100%)	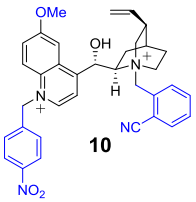 **10** (546)	$[M\text{-}H]^+$ (*m/z* 545, 35%) $[M^{2+}\text{-}R_2^+]^+$ (*m/z* 410, 100%) M^{2+} (*m/z* 273, 24%) R_2^+ (*m/z* 136, 55%)
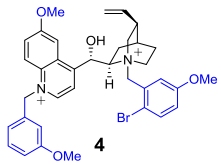 **4** (644)	$[M\text{-}H]^+$ (*m/z* 643, 21%) $[M^{2+}\text{-}R_2^+]^+$ (*m/z* 52, 100%) R_2^+ (*m/z* 121, 90%)	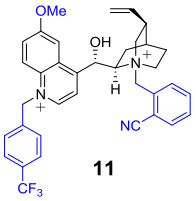 **11** (569)	$[M\text{-}H]^+$ (*m/z* 568, 27%) $[M^{2+}\text{-}R_2^+]^+$ (*m/z* 410, 100%) M^{2+} (*m/z* 284, 22%) R_2^+ (*m/z* 159, 78%)
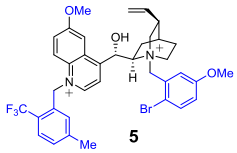 **5** (696)	$[M\text{-}H]^+$ (*m/z* 695, 52%) $[M^{2+}\text{-}R_2^+]^+$ (*m/z* 523, 73%) $[M^{2+}\text{-}R_1^+]^+$ (*m/z* 497, 100%) M^{2+} (*m/z* 347, 90%) R_1^+ (*m/z* 198, 47%) R_2^+ (*m/z* 173, 91%)	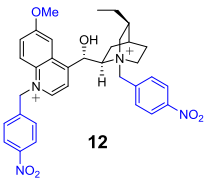 **12** (598)	$[M\text{-}H]^+$ (*m/z* 597, 62%) $[M^{2+}\text{- } R_1^+ \text{ or } R_2^+]^+$ (*m/z* 385, 100%) M^{2+} (*m/z* 299, 44%) R_1^+ or R_2^+ (*m/z* 136, 40%)
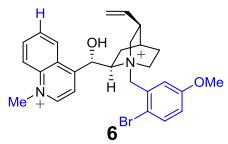 **6** (508)	$[M\text{-}H]^+$ (*m/z* 507, 15%) $[M^{2+}\text{-}R_1^+]^+$ (*m/z* 309, 100%) R_1^+ (*m/z* 198, 43%)	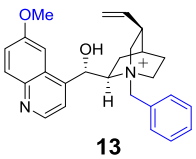 **13** (415)	M^+ (*m/z* 415, 100%) $[M^+\text{-}R_1^+ + H^+]^+$ (*m/z* 325, 62%)
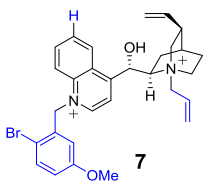 **7** (534)	$[M\text{-}H]^+$ (*m/z* 533, 17%) $[M^{2+}\text{-}H^+\text{-}R_2^+\text{+}H^+]^+$ (*m/z* 335, 100%) R_2^+ (*m/z* 198, 35%)	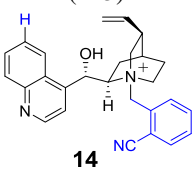 **14** (410)	M^+ (*m/z* 410, 100%) $[M^+\text{-}R_1^+ + H^+]^+$ (*m/z* 295, 35%) $[M^+\text{+}H^+]^{2+}$ (*m/z* 205, 30%) R_1^+ (*m/z* 116, 29%)

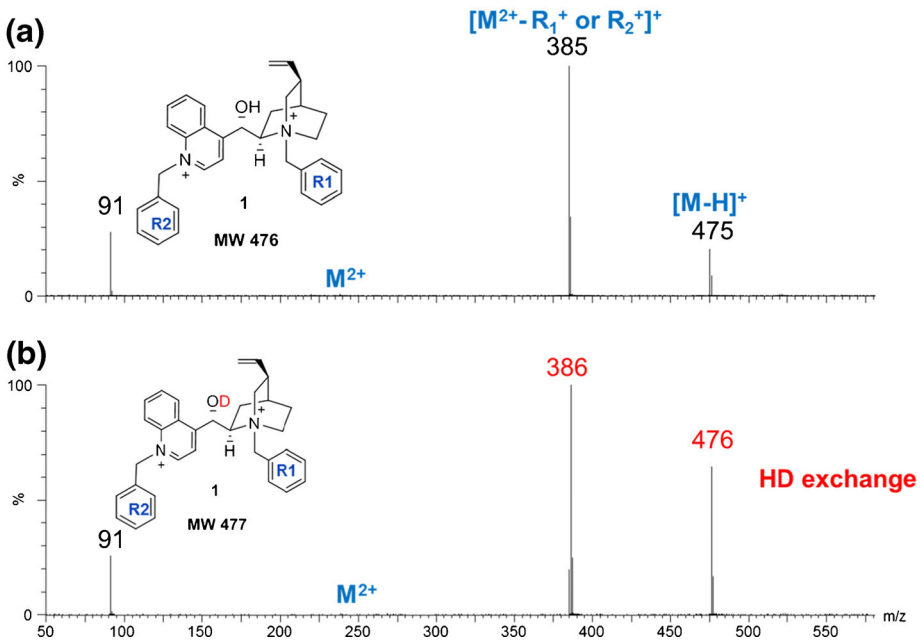

Figure 2. (**a**) MS and (**b**) H/D exchange spectra of compound **1**

did not increase the amount of doubly charged ion M^{2+}. All PTC compounds with bisquaternized ammonium centers produced the Hofmann elimination product ions $[M - H]^+$. The relative abundance of the $[M - H]^+$ ion was about 30%. Interestingly, no Hofmann elimination product was found for compounds **13**–**14**, which only have one quinuclidine ammonium center. These observations suggested that the major driving force for the extensive in-source fragmentation of the PTCs was strong Columbic repulsion between the two charged sites. Compound **1** was selected as an example to illustrate the MS and MS/MS fragmentation pattern since all other PTC derivatives with different R_1 to R_3 groups displayed similar MS patterns. As shown in Figure 2, $[M^{2+} - R_1^+$ or $R_2^+]^+$ with *m/z* 385 was the base peak in the MS spectrum. The relative abundance of the doubly charged ion M^{2+} with *m/z* 238 was only about 2%. The relative abundance of $[M - H]^+$ product ion was about 30%.Similarly, lowering of both ESI and cone voltage did not increase the relative abundance of doubly charged ions in MS spectrum of **1**. Next, efforts were made to locate where the in-source fragmentation was occurring within the API interface.

Is the ESI Probe or MS Inlet Responsible for Inducing In-Source Fragmentation of PTCs?

In order to understand the possible location(s) for in-source fragmentation, three experiments were performed. The first experiment was the temperature variation study of the ESI

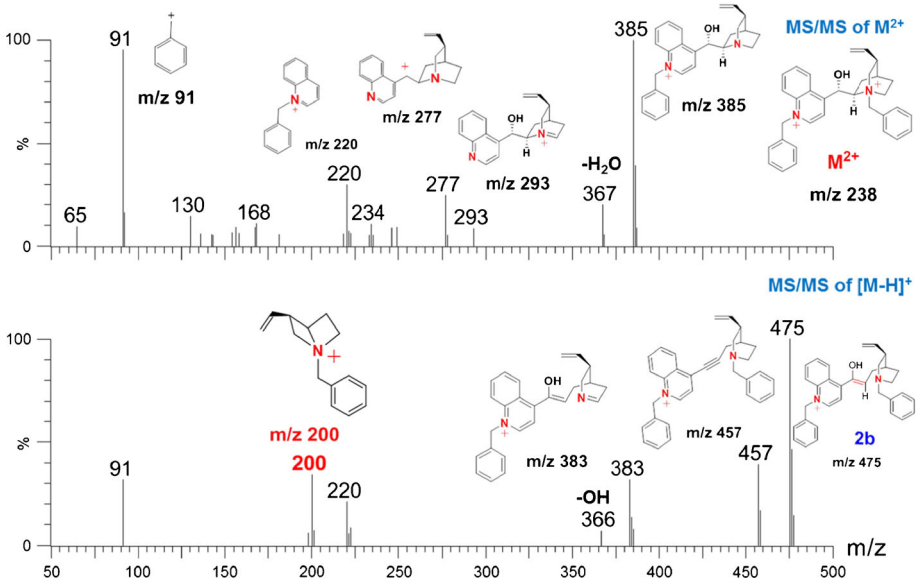

Figure 3. MS/MS on M^{2+} with *m/z* 238 of compound **1 (top)** and $[M - H]^+$ with *m/z* 475 **(bottom)**

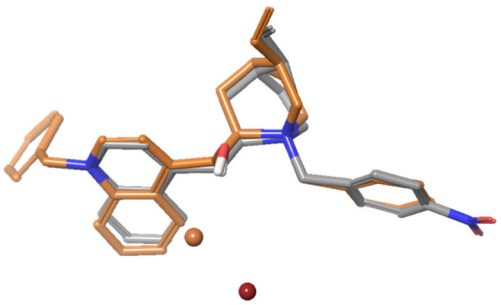

Figure 4. Calculated low energy conformation of **1** (orange) overlaid onto the small molecule crystal structure (CCDC 1479610) of a close analogue (gray) (heavy atom RMSD~0.3 Å, only the quinuclidine bromide is shown). The hydrogen bonding interaction between the OH group and quinuclidine bromide anion is evident for **1**, while the crystal interactions induce a shift of the anion (orange to brown)

probe and ion inlet. The ESI desolvation gas temperature was lowered from 350 °C to 40 °C and the source temperature was also lowered to 40 °C. However, low desolvation gas and source temperature did not change the MS spectrum of **1** (Supplementary Figure S1 in Supporting Information). The second experiment was NMR confirmation of the ESI spray analyte. A sample of **1** was dissolved in ACN and was directly infused through the (+)-ESI probe. All the analyte was collected by a glass vial before it entered the MS inlet. The collected sample was analyzed by NMR, which showed the collected fraction to be identical to compound **1**. These two experiments indicated that the ESI spray alone did not induce fragmentation. The second experiment employed direct infusion of **1** under negative ESI conditions. The bromide anion adduct of the intact PTC dibromo salt was observed under negative ESI conditions when the sample was dissolved in ACN (Supplementary Figure S2), indicating the molecule had not fragmented before it entered the ESI. Hence, it is likely that the electrostatic interaction between the negatively charged bromide anion and the positively charged ion path of the MS inlet induced dissociation of the bromide/ammonium bond.

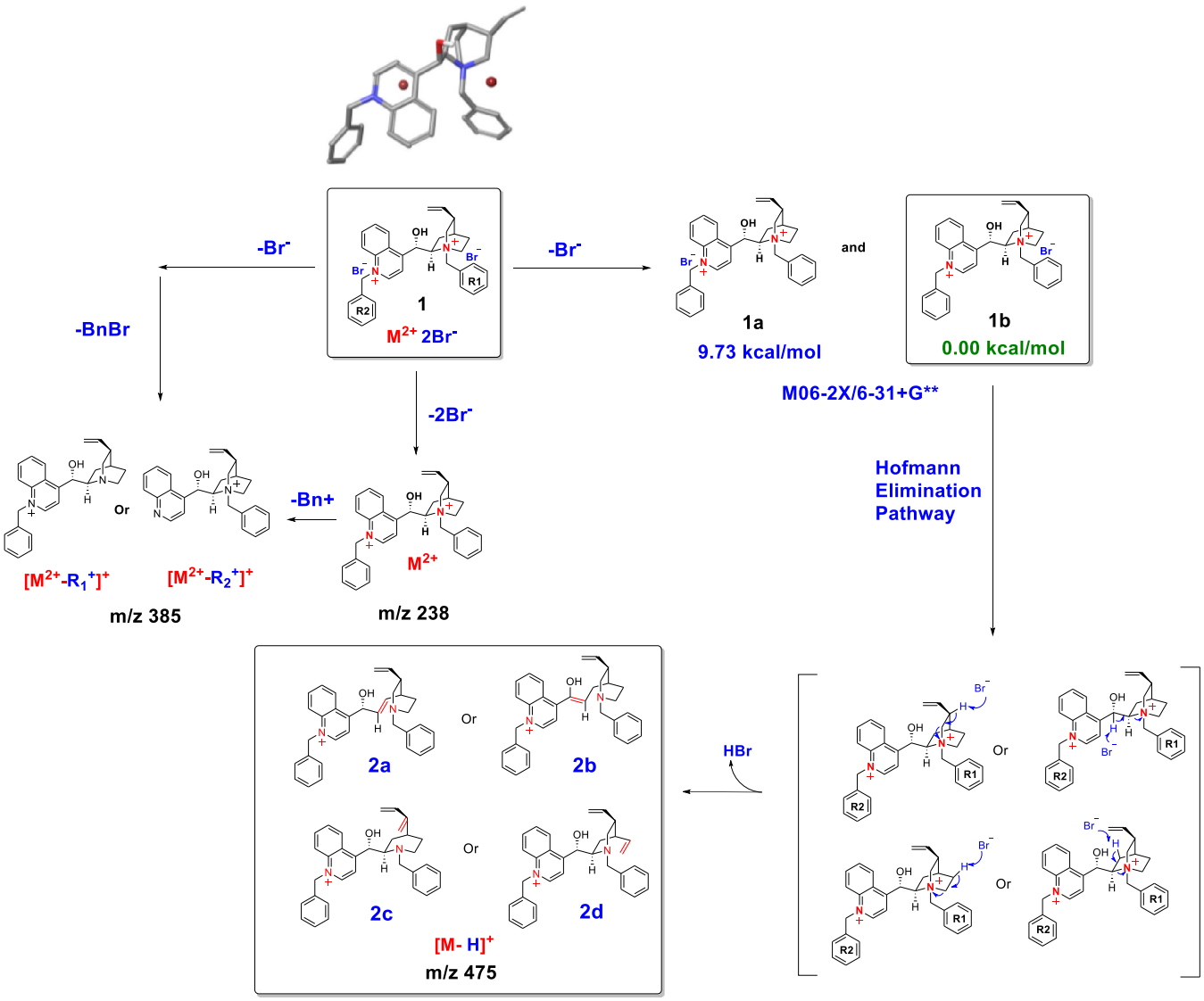

Figure 5. Proposed in-source fragmentation pathway of **1**

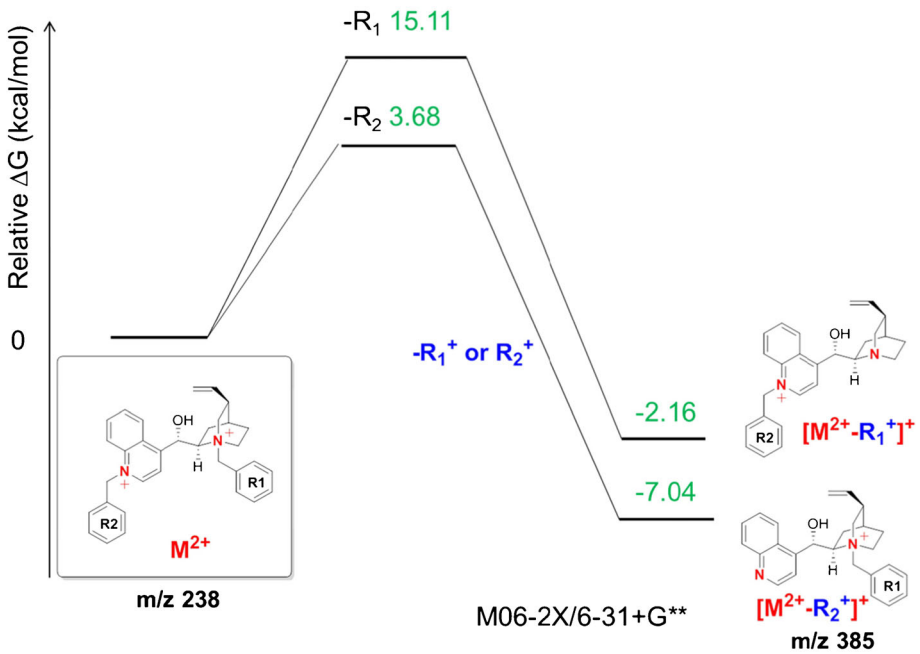

Figure 6. Reaction profile for loss of benzyl cations from the doubly charged cation M^{2+} (products do not include benzyl cation for clarity)

However, due to the potential charge–charge repulsion between the two ammonium cations, the second bromide anion was likely to leave as a neutral molecule such as HBr or benzyl bromide (BnBr) rather than in the anionic form.

MS/MS and H/D Exchange Experiments Reveal the Position of the Double Bond in the Hofmann Elimination Product Ion

For the H/D exchange experiment, the sample was dissolved in 50% D_2O/ACN before direct infusion MS analysis. Hence, all the exchangeable protons such as hydroxyl group in the molecule of interest were expected to be replaced by deuterium. Based on the H/D exchange data (Figure 2), deuterium was still present in the product ions $[M^{2+} - R_1^+$ or $R_2^+]^+$ and $[M - H]^+$, indicating that the hydroxyl group was intact in the $[M - H]^+$ ion. MS/MS was performed on the $[M - H]^+$ ion with *m/z* 475 and M^{2+} ion with *m/z* 238. As shown in Figure 3, the benzyl quinolinium fragment ion, *m/z* 220, was found in the MS/MS spectra of both $[M - H]^+$ and M^{2+}, indicating that the additional proton loss was not occurring on the quinolone part of the molecule. The fragment ion with *m/z* 385 of M^{2+} and *m/z* 383

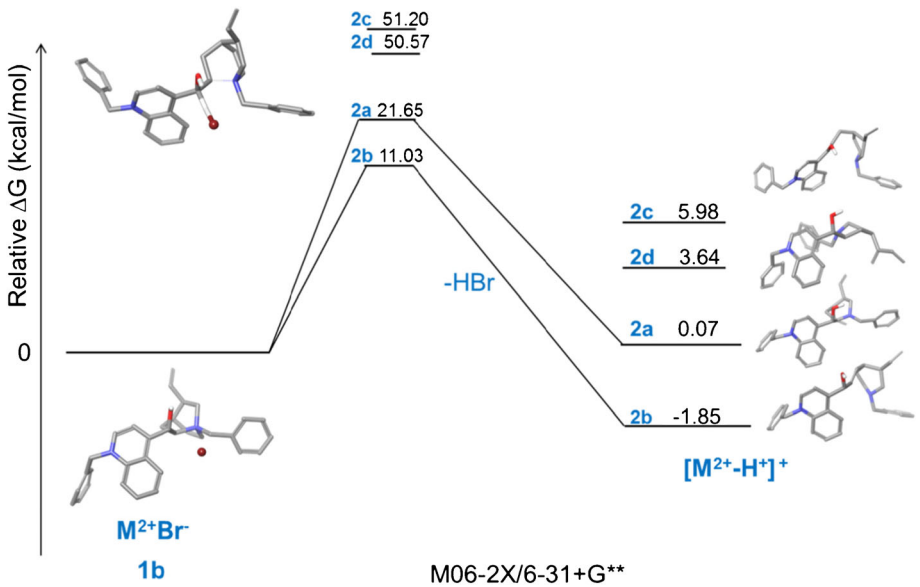

Figure 7. Reaction pathway for the four possible Hofmann elimination product ions **a** to **d** starting from **1b** of the transition state for formation of **b** is shown, in which the Br anion and the ammonium cation are syn-periplanar

of $[M - H]^+$ established that the proton loss was coming from the quinuclidine part of the molecule. Further H/D exchange followed by MS/MS (Supplementary Figure S3) also indicated that the hydroxyl group was present in the fragment ions observed at *m/z* 383 and *m/z* 385 and was not involved in the process of forming the $[M - H]^+$ ion. The MS/MS of the doubly charged ion M^{2+} did not yield the Hofmann elimination product ions $[M - H]^+$. Taken together, these results support Hofmann elimination occurring on the quinuclidine.

Proposed MS In-Source Fragmentation Mechanisms of PTCs

The proposed gas-phase fragmentation mechanism was supported by DFT calculations. We first compared several DFT functionals (B3LYP, B3LYP-D2, B3LYP-D3, M06-2X) and basis sets (6-31G**, 6-31+G**, LANL2DZ, SDD) to assess their ability to replicate the crystal structure of an analogue of **1**. We identified the M06-2X functional and 6-31+G** basis set with the LANL2DZ basis and effective core potential on Br as the optimal combination, given its good agreement with the crystal data. As shown in Figure 4, the calculated low energy conformation of **1** overlaid well with the crystal structure of an analogue. The crystallographic Br anion and the DFT Br anion are separated by a distance of 2.77 Å. This difference is likely due to the presence of a water molecule in the crystal, which is oriented (O-Br distance 3.59 Å, HO-Br angle 154°) to interact with the anion.

The proposed in-source fragmentation pathways for compound **1** are summarized in Figure 5. Under positive ESI, the most likely pathway to form the base peak *m/z* 385 is through bromide anion loss followed by neutral loss of BnBr or HBr in the gas phase. The BnBr and HBr eliminations may be driven by two factors: (1) the resulting singly charged product ion *m/z* 385 is lower in energy compared with the doubly charged ion *m/z* 238 (Figure 6); (2) since ionic bond cleavage is calculated to be endothermic in the gas phase, concerted HBr or BnBr elimination could substantially lower the transition state energy compared with Br anion loss alone [32, 33]. The other pathway to form *m/z* 385 was through benzyl cation loss from the doubly charged *m/z* 238. The calculation results indicated that losing a benzyl cation, **R1,** was more favorable than the loss of **R2** in the case of compound **1** (Figure 5). Fragmentation leads to both product ions being identified, as shown in Table 1.

*Gas Phase Hofmann Elimination of **1***

Solution Hofmann elimination usually involves the concerted bimolecular E2 elimination of the least substituted β proton [34]. In the transition state for Hofmann elimination in solution, the β proton and the quaternary ammonium cation (leaving group) are anti-periplanar [34]. Bulkiness of the quaternary ammonium cation is expected to cause energetically unfavorable gauche interactions with substituents on the adjacent carbon. In order to avoid gauche interactions, elimination proceeds via the least substituted β proton.[35] In the case of gas phase Hofmann eliminations in the studied PTCs, cations **1a** and **1b** resulting from loss of one bromine anion represent the two possible intermediates that can further undergo elimination (Figure 5). Calculation of relative energies indicates **1b** (0.0 kcal/mol) is more stable than **1a** (9.73 kcal/mol) due to hydrogen bonding between the OH group and the Br anion (Figure 4). During the ionization process, the quinolone bromide anion is more likely to be lost first to form **1b** followed by loss of the quinuclidine bromide anion as a neutral molecule. For the gas-phase Hofmann elimination of **1b**, the most likely basic anion available to abstract a β proton was the bromide anion. Moreover, there were four different β hydrogens available for elimination leading to four possible $[M - H]^+$ product ions (**2a**–**2d**) (Figure 5).

Reaction profiles for Hofmann elimination reactions (**2a**–**2d**) were calculated at M06-2X/6-31+G** level of theory (Figure 7). The results indicated product ion **2b** had the lowest activation barrier and lowest relative product energy followed by **2a**, **2d**, and **2c**. Calculations are in good agreement with the

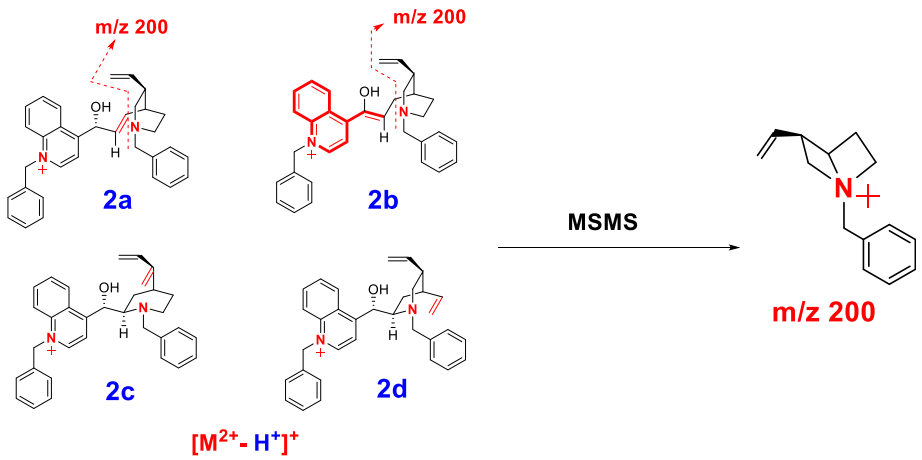

Figure 8. Only Hofmann elimination product **2a** and **2b** are able to form product fragment ion *m/z* 200. The conjugation between the olefin and quinolinium is highlighted in bold

MS/MS data in Figure 3. A key fragment ion with *m/z* 200 could only be formed from Hofmann elimination product ions **2a** and **2b** but not from **2c** and **2d** (Figure 8). Taken together, experimental fragmentation patterns and computed energetics indicate product ion **2b** is the most likely gas-phase Hofmann elimination product. Interestingly, according to standard interpretation of solution Hofmann eliminations, product **2a** should be the major elimination product since **2a** is formed through elimination of a β proton on the less-hindered secondary carbon, whereas product **2b** is formed through elimination of a β proton on the more hindered tertiary carbon. There are two possible explanations for this: (1) product ion **2b** is more stable than **2a** due to conjugation between the olefin and aromatic ring of the quinolinium (Figure 7); (2) the transition state leading to product **2b** was lower than **2a** since the bromide anion was closer to the tertiary β hydrogen due to a hydrogen bonding interaction with the hydroxyl group. The transition state calculations also indicate that the elimination proceeds through a unimolecular E_i elimination pathway [36], in which the bromide anion and the ammonium cation leaving group are syn-periplanar. The unimolecular nature of the gas-phase elimination reaction [37–40] and the tight coordination between the bromide anion and the ammonium cation in the gas phase leads to the formation of **1b** as the major gas phase Hofmann elimination product of **1**.

Conclusions

In this present study, the in-source fragmentation pathways of 14 doubly quaternized cinchona-alkaloid-based phase-transfer catalysts (**1–14**) were studied under (+)-ESI. The results showed all compounds give $[M^{2+} - R_1^+$ or $R_2^+]^+$, $[M - H]^+$, and M^{2+} ions in the MS spectra. The likely driving force for the formation of these fragment ions was to mitigate the strong Columbic repulsion in the gas phase between the two quaternized ammonium cations. The mechanism for formation of the gas-phase Hofmann elimination $[M - H]^+$ products was elucidated by application of HRMS/MS, H/D exchange, and DFT calculation using compound **1** as an example. The proposed formation of **2b** as the major Hofmann elimination product was supported by both HRMS/MS and DFT calculations. Product ion **2b** is proposed to form through a concerted unimolecular E_i elimination pathway rather than the bimolecular E2 elimination pathway for common solution Hofmann eliminations. The mechanistic understanding of this unusual in-source fragmentation may aid in the interpretation of structural elucidation efforts for compounds with similar structures.

Acknowledgements

The authors thank Gary Martin, Josep Sauri, and Christopher Welch for their insightful discussions.

References

1. Yeboah, E.M.O., Yeboah, S.O., Singh, G.S.: Recent applications of cinchona alkaloids and their derivatives as catalysts in metal-free asymmetric synthesis. Tetrahedron. Lett. **67**, 1725–1762 (2011)
2. Tropical plants database available at http://www.rain-tree.com/plants.htm. Raintree Nutrition: Carson City. Accessed April 2016
3. Xiang, B., Belyk, K.M., Reamer, R.A., Yasuda, N.: Discovery and application of doubly quaternized cinchona-alkaloid-based phase-transfer catalysts. Angew. Chem. Int. Ed. **53**, 8375–8378 (2014)
4. Cao, J., Li, C., Zhang, Z., Xu, C., Yan, J., Cui, F., Hu, C.: Intriguing role of a 5 quaternary ammonium cation in the dissociation chemistry of Keggin polyoxometalate anions. J. Am. Soc. Mass Spectrom. **23**, 366–374 (2012)
5. Cydzik, M., Rudowska, M., Stefanowicz, P., Szewczuk, Z.: The competition of charge remote and charge directed fragmentation mechanisms in quaternary ammonium salt derivatized peptides—an isotopic exchange study. J. Am. Soc. Mass Spectrom. **22**, 2103–2107 (2011)
6. Amy, J.W., Baitinger, W.E., Cooks, R.G.: Building mass spectrometers and a philosophy of research. J. Am. Soc. Mass Spectrom. **1**, 119–128 (1990)
7. Cooks, R.G., Busch, K.L., Glish, G.L.: Mass spectrometry: capabilities and potentials. Science **222**, 273–291 (1983)
8. Barcelo, D., Durand, G., Vreeken, R.J.: Determination of quaternary amine pesticides by thermospray mass spectrometry. J. Chromatogr. A **647**, 271–277 (1993)
9. Tondeur, Y., Sovocool, G.W., Mitchum, R.K., Niederhut, W.J., Donnelly, J.R.: Use of FAB MS/MS for analysis of quaternary amine pesticide standards. Biomed. Environ. Mass Spectrom. **14**, 733–736 (1987)
10. Evan, C.S., Startin, J.R., Goodall, D.M., Keely, B.J.: Optimization of ion trap parameters for the quantification of chlormequat by liquid chromatography/mass spectrometry and the application in the analysis of pear extracts. Rapid Commun. Mass Spectrom. **14**, 112–117 (2000)
11. Taguchi, V.Y., Jenkins, S.W.D., Crozier, P.W., Wang, D.T.: Determination of diquat and paraquat in water by liquid chromatography-(electrospray ionization) mass spectrometry. J. Am. Soc. Mass Spectrom. **9**, 830–839 (1998)
12. Marr, J.C., King, J.B.: A simple high performance liquid chromatography/ionspray tandem mass spectrometry method for the direct determination of paraquat and diquat in water. Rapid Commun. Mass Spectrom. **11**, 479–483 (1997)
13. Castro, R., Moyano, E., Galceran, M.T.: Ion-pair liquid chromatography–atmospheric pressure ionization mass spectrometry for the determination of quaternary ammonium herbicides. J. Chromatogr. A **830**, 145–154 (1999)
14. Song, X., Budde, W.L.: Capillary electrophoresis-electrospray mass spectra of the herbicides paraquat and diquat. J. Am. Soc. Mass Spectrom. **7**, 981–984 (1996)
15. Moyano, E., Games, D.E., Galceran, M.T.: Determination of quaternary ammonium herbicides by capillary electrophoresis/mass spectrometry. Rapid Commun. Mass Spectrom. **10**, 1379–1385 (1996)
16. Pashynska, V.A., Kosevich, M.V., Gömöry, A., Szilágyi, Z., Vékey, K., Stepanian, S.G.: On the stability of the organic dication of the bisquaternary ammonium salt decamethoxinum under liquid secondary ion mass spectrometry. Rapid Commun. Mass Spectrom. **19**, 785–797 (2005)
17. Wang, X., Sha, Y., Li, R.: Fragmentation patterns of novel dispirocyclopiperazinium dibromides with strong analgesic activity under electrospray ionization tandem mass spectrometry conditions. Rapid Commun. Mass Spectrom. **18**, 829–833 (2004)
18. Evans, C.S., Startin, J.R., Goodall, D.M., Keely, B.J.: Tandem mass spectrometric analysis of quaternary ammonium pesticides. Rapid Commun. Mass Spectrom. **15**, 699–707 (2001)
19. Jiang, W., Schalley, C.A.: Tandem mass spectrometry for the analysis of self-sorted pseudorotaxanes: the effects of Coulomb interactions. J. Mass Spectrom. **45**, 788–798 (2010)
20. Juang, Y.M., She, T.F., Chen, J.Y., Lai, C.C.: Comparison of CID versus ETD-based MS/MS fragmentation for the analysis of doubly derivatized steroids. J. Mass Spectrom. **48**, 1349–1356 (2010)
21. Ramos, C.I., Santana-Marques, M.G., Ferrer Correia, A.J., Tomé, J.P., Alonso, C.M., Tomé, A.C., Neves, M.G., Cavaleiro, J.A.: Reduction and

adduct formation from electrosprayed solutions of porphyrin salts. J. Mass Spectrom. **43**, 806–813 (2008)
22. Vijay Darshan, D., Chandar, B.G.N., Srujan, M., Chaudhuri, A., Prabhakar, S.: Electrospray ionization tandem mass spectrometry study of six isomeric cationic amphiphiles with ester/amide linker. Rapid Commun. Mass Spectrom. **28**, 1209–1214 (2014)
23. Donkuru, M., Chitanda, J.M., Verrall, R.E., El-Aneed, A.: Multi-stage tandem mass spectrometric analysis of novel β-cyclodextrin-substituted and novel bis-pyridinium gemini surfactants designed as nanomedical drug delivery agents. Rapid Commun. Mass Spectrom. **28**, 757–772 (2014)
24. Frisch, M.J., Trucks, G.W., Schlegel, H.B., Scuseria, G.E., Robb, M.A., Cheeseman, J.R., Scalmani, G., Barone, V., Mennucci, B., Petersson, G.A., Nakatsuji, H., Caricato, M., Li, X., Hratchian, H.P., Izmaylov, A.F., Bloino, J., Zheng, G., Sonnenberg, J.L., Hada, M., Ehara, M., Toyota, K., Fukuda, R., Hasegawa, J., Ishida, M., Nakajima, T., Honda, Y., Kitao, O., Nakai, H., Vreven, T., Montgomery Jr., J.A., Peralta, J.E., Ogliaro, F., Bearpark, M., Heyd, J.J., Brothers, E., Kudin, K.N., Staroverov, V.N., Kobayashi, R., Normand, J., Raghavachari, K., Rendell, A., Burant, J.C., Iyengar, S.S., Tomasi, J., Cossi, M., Rega, N., Millam, J.M., Klene, M., Knox, J.E., Cross, J.B., Bakken, V., Adamo, C., Jaramillo, J., Gomperts, R., Stratmann, R.E., Yazyev, O., Austin, A.J., Cammi, R., Pomelli, C., Ochterski, J.W., Martin, R.L., Morokuma, K., Zakrzewski, V.G., Voth, G.A., Salvador, P., Dannenberg, J.J., Dapprich, S., Daniels, A.D., Farkas, Ö., Foresman, J.B., Ortiz, J.V., Cioslowski, J., Fox, D.J.: Gaussian 09, Revision E.01. Gaussian, Inc, Wallingford (2009)
25. Zhao, Y., Truhlar, D.G.: The M06 Suite of Density Functionals for main group thermochemistry, thermochemical kinetics, noncovalent interactions, excited states, and transition elements: two new functionals and systematic testing of four M06-class functionals and 12 other functionals. Theor. Chem. Account **120**, 215–241 (2006)
26. Wadt, W.R., Hay, P.J.: Ab initio effective core potentials for molecular calculations. Potentials for the transition metal atoms Sc to Hg. J. Chem. Phys. **82**, 270 (1985)
27. Wadt, W.R., Hay, P.J.: Ab initio effective core potentials for molecular calculations. Potentials for main group elements Na to Bi. J. Chem. Phys. **82**, 284 (1985)
28. Wadt, W.R., Hay, P.J.: Ab initio effective core potentials for molecular calculations. Potentials for K to Au including the outermost core orbitals. J. Chem. Phys. **82**, 299 (1985)
29. Rassolov, V.A., Ratner, M.A., Pople, J.A., Redfern, P.C., Curtiss, L.A.: 6-31G* basis set for third-row atoms. J. Comput. Chem. **22**, 976–984 (2001)
30. Schrödinger Release 2016-1: Maestro, Version 10.5. Schrödinger, LLC: New York, NY (2016)
31. AGUI program: available at: www.semichem.com. Semichem, Inc.: Shawnee, KS (2016)
32. Duarte, F., Gronert, Scott, Kamerlin, S.C.L.: Concerted or stepwise: how much do free-energy landscapes tell us about the mechanisms of elimination reactions? J. Org. Chem. **79**, 1280–1288 (2014)
33. Meng, Q., Gogoll, A., Thibblin, A.: Concerted and stepwise solvolytic elimination and substitution reactions: stereochemistry and substituent effects. J. Am. Chem. Soc. **119**, 1217–1223 (1997)
34. Cope, A.C., Mehta, A.S.: Mechanism of the Hofmann elimination reaction: an ylide intermediate in the pyrolysis of a highly branched quaternary hydroxide. J. Am. Chem. Soc. **85**, 1949–1952 (1963)
35. von Doering, W.E., Meislich, H.: Mechanism of the Hofmann elimination. J. Am. Chem. Soc. **74**, 2099–2100 (1952)
36. Saha, S., Dua, A.: Stochastic Lindemann kinetics for unimolecular gas-phase reactions. J. Phys. Chem. A **117**, 7661–7669 (2013)
37. Tajima, S., Watanabe, D., Ubukata, M., Hirol, Y., Nakajima, S., Nibbering, N.M.M.: Unimolecular gas-phase reactions of methyl and ethyl trifluoroacetoacetates upon electron ionization. Int. J. Mass Spectrom. **219**, 475–483 (2002)
38. Gronert, S.: Gas-phase studies of the competition between substitution and elimination reactions. Acc. Chem. Res. **36**, 848–857 (2003)
39. Gronert, S., Fong, L.M.: Structural effects on the gas phase reactivity of organic salt complexes: substitution versus Hofmann elimination. Aust. J. Chem. **56**, 379–383 (2003)
40. Gronert, S., Azebu, J.: Reactions of gas-phase salts: substitutions and eliminations in complexes containing a di-anion and a tetra-alkylammonium cation. Org. Lett. **1**, 503–506 (1999)